Optimization of polarization spectroscopy for rubidium D lines*

Sun Jian-Fang(孙剑芳), Yin Shi-Qi(尹士奇), Xu Zhen(徐 震)†, Hong Tao(洪 涛), and Wang Yu-Zhu(王育竹)‡

Key Laboratory for Quantum Optics, Center for Cold Atom Physics, Shanghai Institute of Optics and Fine Mechanics, Chinese Academy of Sciences, Shanghai 201800, *China*

(Received 20 July 2012; revised manuscript received 27 August 2012)

Polarization spectroscopy of the D lines of rubidium atoms is investigated experimentally, especially with different pump powers and cell temperatures. We find that there are four candidate transitions suitable for frequency stabilization, and optimal pump powers and cell temperatures are also presented to obtain a perfect signal with maximal amplitude and slope. The optimal signal is insensitive to the fluctuations of laser power and the temperature, which can enhance the performance of frequency locking.

Keywords: polarization spectroscopy, pump power, temperature

PACS: 42.62.Fi, 32.80.Xx, 51.70.+f **DOI:** 10.1088/1674-1056/22/2/024207

1. Introduction

External cavity semiconductor laser (ECDL) is widely used in atomic physics, especially for laser cooling and trapping of neutral atoms in gases,[1–4] metrology, and atomic clocks.[5,6] Frequency stabilization is of great importance to the performance of ECDL, because it is very sensitive to ambient temperature, electric current, and mechanical vibration. In the experiments of cold atomic physics, the laser is often locked at the narrow transitions of atomic gases. The Doppler-free techniques, such as saturated absorption spectroscopy (SAS),[7] have been widely utilized in the laser's frequency locking. In SAS, the laser can only be side-locked, which makes frequency locking very susceptible to the instability of the power of the probe laser. Therefore frequency modulation spectroscopy is always used to produce a dispersion-like signal for peak-locking, but it requires more electronic devices.[7]

Alternatively, modulation free dispersion-like spectroscopy is also employed in the laser frequency stabilization, such as dichroic atomic vapor laser lock (DAVLL),[8–10] and polarization spectroscopy (PS).[11–15] In DAVLL, an optimal uniform magnetic field is required to introduce appropriate Zeeman shifts.[16,17] For example, the optimal magnetic field is about 120 Gs (1 Gs=10^{-4} T) for the DAVLL spectrum of the rubidium (Rb) 87 atom's D2 line.[17] Unlike DAVLL, the magnetic field is not employed in PS.

First proposed by Wieman and Hänsch in 1976,[11] PS has better signal-to-noise ratio (S/N) than saturated absorption spectroscopy[7] and has a locking precision less than 1 MHz.[18] Much theoretical[12,13] and experimental[19–21] effort has been made for over three decades. In this work, the polarization spectroscopy of Rb atoms D line is investigated. The optimal temperatures are found to improve the S/N ratio and stability. At the optimal temperature, the amplitude and slope of PS signals are insensitive to the temperature variation, which can be used to stabilize the laser frequency. The relationship of the PS signal with the power of the pump laser has also been studied.

2. Principle of polarization spectroscopy

In PS, a linearly polarized probe laser propagates through the Rb cell along the z axis, meanwhile a circularly polarized pump laser counter-propagates and overlaps with the probe beam to generate the birefraction effect. The polarization of the probe beam has an angle of $\theta \simeq \pi/4$ with respect to the x axis. Choosing the z axis as the quantization axis, the linear polarized probe beam can be decomposed into σ^+ and σ^- circular polarization components with equal amplitude. The refractive index and absorption coefficient of rubidium vapor are $n_\pm$ and $\alpha_\pm$ for $\sigma^\pm$ components of the probe beam, respectively. The complex refractive index introduced by the cell windows is denoted as $\mu_\pm + \mathrm{i}\nu_\pm$. Then the electric field after travelling through the Rb cell is[13]

$$\begin{aligned} \boldsymbol{E} = \frac{E_0}{\sqrt{2}}[&-\hat{\varepsilon}_+ \mathrm{e}^{-\alpha_+ L/2}\mathrm{e}^{\mathrm{i}(kn_+L-\theta)}\mathrm{e}^{\mathrm{i}kL(\mu_+ + \mathrm{i}\nu_+)} \\ &+\hat{\varepsilon}_- \mathrm{e}^{-\alpha_- L/2}\mathrm{e}^{\mathrm{i}(kn_-L+\theta)}\mathrm{e}^{\mathrm{i}kL(\mu_- + \mathrm{i}\nu_-)}], \end{aligned} \tag{1}$$

where $\hat{\varepsilon}_\pm = \mp(\hat{x} \pm \mathrm{i}\hat{y})/\sqrt{2}$, and k is the wave vector. Rewriting the refraction indexes and absorption coefficients as $\eta_\pm = \eta \pm \Delta\eta/2$, where $\eta = n, \alpha, \mu, \nu$, the intensity difference can be written as

$$\Delta I = I_x - I_y = I_0 \sin\left[\frac{\pi}{2} - 2\theta + kL(\Delta n + \Delta\mu)\right], \tag{2}$$

*Project supported by the Research Project of Shanghai Science and Technology Commission (Grant No. 09DJ1400700), the National 973 Program of China (Grant No. 2011CB921504), and the National Natural Science Foundation of China (Grant No. 10974211).

†Corresponding author. E-mail: xuzhen@siom.ac.cn

‡Corresponding author. E-mail: yzwang@mail.shcnc.ac.cn

© 2013 Chinese Physical Society and IOP Publishing Ltd

where $I_0 = \frac{1}{2}\varepsilon_0 c E_0^2 \exp[-(\alpha + 2k\nu)L]$ is the intensity of the probe beam after the Rb cell. We choose $\theta = \pi/4 + (kL/2)\Delta\mu$. Then for small Δn Eq. (2) is simplified as[13]

$$\Delta I \cong I_0 kL\Delta n. \tag{3}$$

In the above equation, Δn can be obtained by Kramers–Kronig relation as follows:[22]

$$\Delta n = \frac{c}{\omega_0}\Delta\alpha_0 \frac{x}{1+x^2}, \tag{4}$$

where, $x = 2\Delta/\Gamma$, Δ is laser detuning and Γ is natural linewidth. $\Delta\alpha_0$ is the absorption coefficient difference between two circularly polarized components of the probe beam at resonance. From Eqs. (3) and (4), we arrive at

$$\Delta I = A \times \frac{x}{1+x^2} \times N\Delta s \times \exp\left(-\frac{1}{2}N(s_+ + s_-)L\right), \tag{5}$$

where N is the atomic density of the corresponding Zeeman state, $A = \frac{1}{2}\varepsilon_0 c E_0^2 L \exp(-2k\nu L)$, and $\Delta\alpha_0 = \alpha_+ - \alpha_- = N(s_+ - s_-) = N\Delta s$. Here $s_\pm$ and Δs are the scattering cross section of $\sigma^\pm$ light and the difference of scattering cross sections with the $\sigma^\pm$ light of the corresponding Zeeman state, respectively.

As shown in Eq. (5), the PS signal has a natural dispersion shape with zero background. The signal is proportional to Δs, and has a maximum value at a suitable N. For the PS, no magnetic field is needed and the Zeeman states are still degenerate, but for different Zeeman ground states, the Δs differs. In this work, several transitions that have large Δs are chosen, and the corresponding PS signals change with the temperature of the Rb cell and the power of the pump beam are measured.

3. Experiment setup

The schematic diagram of experimental setup for both D1 and D2 lines is shown in Fig. 1. Two ECDL lasers (Sacher Lasertechnik TEC 500 and New Focus Vortex 6000) are used for D1 and D2 lines, respectively. The former has a wavelength of 795 nm and a beam diameter of 2 mm, while for the latter they are 780 nm and 1.5 mm, respectively. We use an isolator to avoid laser feedback. The output beam is split into two beams by PBS1. One is for PS and the other is for SAS as frequency reference. The polarization angle of the probe beam is rotated about $\pi/4$ to the x axis by a half wave plate before PBS3. At this angle, the intensity $I_x = I_y$ in the absence of the pump beam, which can be used as a criterion in the experiment. A Glan prism and a quarter wave plate are used to purify the circular polarization of the pump beam. We use a balanced differential Si-photo-diode to detect the PS signal. The length and diameter of the Rb cell are 50 mm and 25 mm, respectively. A single layer μ-metal is applied to shield the earth?s magnetic field and results in a residual magnetic field lower than 10 mGs. The temperature of the Rb cell can be regulated from room temperature to more than 100 °C with the uncertainty under 1 °C by a heater and a PID module.

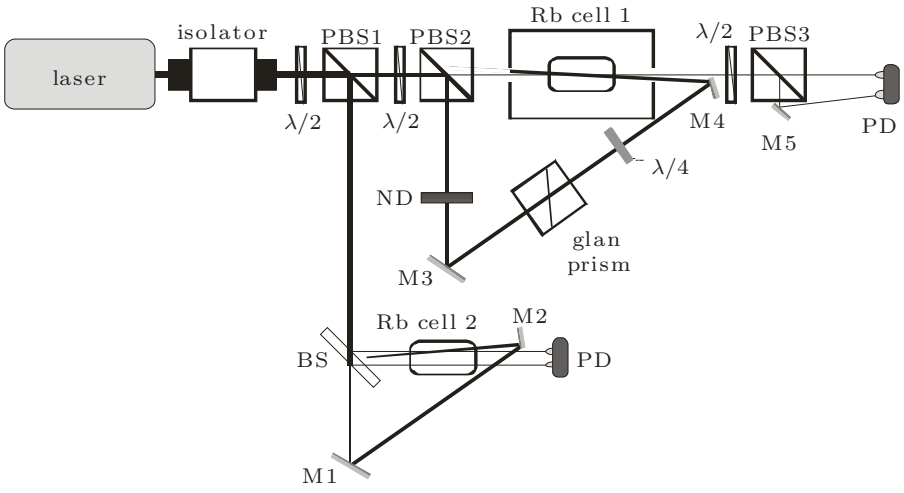


Fig. 1. Schematic plot of experimental setup. ($\lambda/2$: half-wave plate, PBS: polarizing beamsplitter, ND: neutral density filter, $\lambda/4$: quarter-wave plate, BS: beamsplitter, PD: photodiodes).

4. Results and discussions

The PS and SAS signals of Rb atoms' D2 line are shown in Fig. 2. The maximum peaks of PS signals are not consistent with SAS, and the amplitude and shape of each PS signal is different. This difference can be attributed to two factors, one is Δs, and the other is the decay channel of the excited energy level. Although the Zeeman states are degenerate in the absence of a magnetic field, they have different absorp-

tion coefficients for the polarized lights of σ^+ and σ^-, which results in different values of $\Delta\alpha$. It should be noted that the difference between the absorption coefficients of σ^+ and σ^- is not related to the Zeeman shift, but is proportional to the difference between the scattering lengths of two polarizations. Therefore $\Delta\alpha$ affects the signal ΔI remarkably (see Eq. (5)). Therefore, to obtain a large PS signal, a proper Zeeman state should be chosen. The PS signal dependence on the decay channel is explicated in Refs. [22] and [23]. As is well known, a good candidate of PS spectra for frequency locking should have a large peak-to-peak amplitude and a large slope. Therefore, for Rb atoms' D2 line, there are two transitions (^{87}Rb $F = 2 \to F' = 3$ and ^{85}Rb $F = 3 \to F' = 4$) more suitable for laser locking, as shown in Fig. 2. We pick and list them in Table 1, as well as the two transitions of D1 line, which are not shown in figures. From the analysis in Section 2, the circularly polarized pump laser plays a central role in polarization spectroscopy, and the temperature also affects the amplitude of the PS signal. Below we will discuss the influence of the pump power and temperature to PS signals.

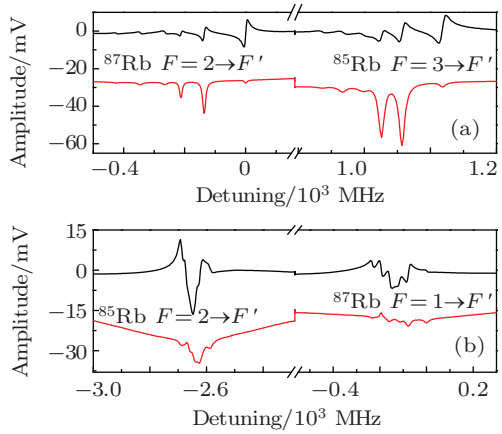


Fig. 2. (color online) PS (black) and SAS (red) signals of Rb atoms' D2 line. In panel (a), we choose the ^{87}Rb $F = 2 \to F' = 3$ transition as zero detuning, while in panel (b), the ^{87}Rb $F = 1 \to F' = 2$ transition is chosen to be zero detuning. The cell temperature is 29 °C, and the pump and probe powers are 17.0 μW and 19.4 μW, respectively. The pump beam is not very strong to avoid power broadening.

Table 1. The optimal temperature range and maximum ratio ($A_{\rm opt}/A_{\rm room}$) of the four transitions.

	Optimal T/°C	($A_{\rm opt}/A_{\rm room}$)
^{87}Rb D2 $F = 2 \to F' = 3$	38∼ 41	1.7
^{87}Rb D1 $F = 2 \to F' = 2$	73∼ 77	17
^{85}Rb D2 $F = 3 \to F' = 4$	25∼ 29	1.03
^{85}Rb D1 $F = 3 \to F' = 3$	57∼ 63	6

First, we give the pump beam effect on the PS signal, which produces the imbalance of the atomic population in different Zeeman states. We measured the PS signal against the power of pump laser of the four transitions. As a paradigmatic example, Fig. 3(a) shows the peak-to-peak amplitude, 3(b) linewidth, and 3(c) slope of the ^{85}Rb D2 line $F = 3 \to F' = 4$ transition. This figure measured at three different probe powers and the amplitudes and slopes are almost proportional to probe powers, while the linewidths are independent of probe powers. In the low pump power region, the amplitude drastically increases with pump power. This is because with increasing pump power, more and more atoms are pumped to $F = 3$, $m_F = 3$ state, which increases the atomic density in this Zeeman state. While in the high pump power region, the amplitude is saturated, because almost all the atoms

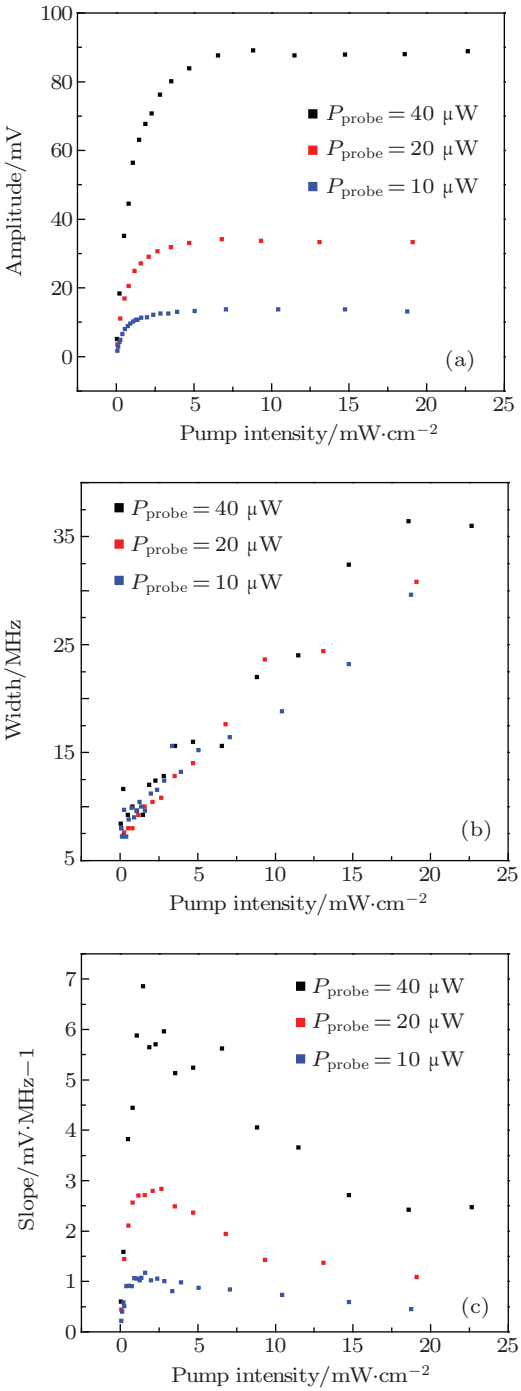


Fig. 3. (color online) Peak-to-peak amplitude (a), linewidth (b), and slope (c) of near zero point of PS signals of ^{85}Rb D2 line $F = 3 \to F' = 4$ against pump intensity. The temperature of the Rb cell is kept at 27 °C. The PS signals are measured at three different probe powers, 10 μW (blue), 20 μW (red), and 40 μW (black), respectively.

are pumped to $m_F = 3$ state as soon as they are in the light field. The linewidth of the PS signal is almost proportional to the pump power due to power broadening. To utilize the PS signal for frequency stabilization, the slope should be larger and insensitive to power jitter, so it is better to keep the pump power at the turning region. At these regions, the slopes are insensitive to pump power, and the amplitudes are also good. We found the turning regions of the slopes are almost the same for different powers of the probe laser. That is similar to other transitions of rubidium D lines in our measurements.

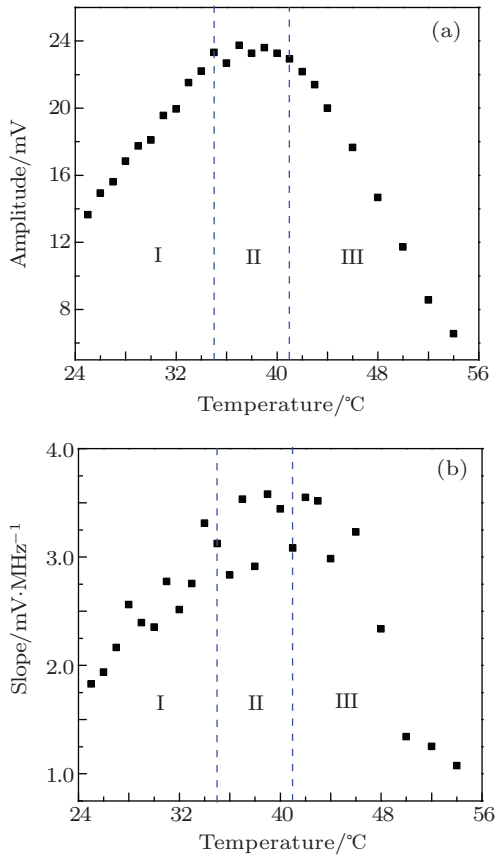


Fig. 4. (color online) Amplitude (a) and slope (b) of PS signal of ^{87}Rb D2 line $F = 2 \rightarrow F' = 3$ against cell temperature. The power of pump and probe are 17 μW and 19.8 μW, respectively.

In the following, we turn to investigate the effect of the temperature on PS and give the optimal temperature for frequency locking. The amplitudes and the slopes of PS spectra for the D2 line $F = 2 \rightarrow F' = 3$ transition with different cell temperatures are measured (see Fig. 4). An appropriate pump power was chosen to avoid power broadening. It is clear that the cell temperature has great influence on the performance of PS spectra, and there is an optimal parameter regime of the cell temperature in which the locking can be operated. We have observed similar dependencies of the amplitude and the slope on the temperature in PS signals. In the regime of low temperature (region I), they both increase monotonously with the temperature. This means that a PS signal can be improved by increasing the cell temperature. The frequency locking, however, cannot operate well at a high temperature (region III), because the two key parameters become too small to lock the laser. At an intermediate temperature (region II), the amplitude and the slope of the signals are both large. Especially, the low temperature-sensitivity of amplitude at intermediate temperatures makes the PS signal more suitable for frequency locking.

The above trend of the amplitude in PS can be explained by the formalism presented in Section 2. For simplicity, we rewrite Eq. (5) as

$$\Delta I = \eta \times N \times \exp(-\beta N), \tag{6}$$

where η, β are temperature-independent parameters, while the atomic density N is determined by the cell temperature. It is shown in Eq. (6) that the signal is not a monotonous function of the atomic density, and we have to characterize its dependence on the temperature in different regimes.

When the temperature is low, the number of atoms in the ground state is small. In this regime, the amplitude of the PS signal is mainly determined by the second term in Eq. (6), rather than the exponential term. With increasing temperature and thus atomic density, the PS signal increases almost linearly, while in the high-temperature regime, the exponential term dominates the PS signal that decreases with N or T remarkably. In region II, the two terms are comparable to each other, so the temperature has little effect on the signal's amplitude. This is the optimal regime for the operation of frequency locking using PS.

We also measured the performance of PS for other candidate transitions and found that the temperature effect is similar to the above observation shown in Fig. 4; however, of course, respective optimal temperatures are different. The optimal temperatures of each transition and the ratios of maximum amplitudes to the amplitudes at room temperature ($A_{\rm opt}/A_{\rm room}$) are listed in Table 1. For these four transitions, the optimal temperatures for the ^{87}Rb D1 (D2) line are higher than for the ^{85}Rb D1 (D2) line, because the abundance of ^{87}Rb in the cell is lower than that of ^{85}Rb. Therefore at higher temperatures, higher N is required in order to obtain the optimal amplitudes for ^{87}Rb atoms. Meanwhile the optimal temperatures for the D1 line are higher than the D2 line for both ^{87}Rb and ^{85}Rb atoms — because there is no closed transition for the D1 line, higher temperature is required to increase the atomic density. So we can expect that D1 lines have larger ($A_{\rm opt}/A_{\rm room}$) as listed in Table 1. This is helpful in maximizing the amplitude and signal-to-noise ratio of the PS signal and enhancing the stability of the PS signal at the optimal cell temperature for laser frequency stabilization.

5. Conclusion

In this paper, we experimentally studied the polarization spectroscopy of rubidium D lines. We chose four suit-

able transitions to study the performance with variations in pump power and temperature. The amplitude of the PS signal drastically increased, and then saturated with increasing pump power, but the linewidth increased almost linearly with increasing pump power due to power broadening. The maximum and flat slope of the PS signal is found at the same pump power with different probe power. By increasing the cell temperature, the PS signal can be enhanced with optimal temperature. The amplitude of the PS signal is maximized at optimal temperature and has a flat region. At the optimal pump power and cell temperature, both the amplitude and the slope of the PS signal are insensitive to the fluctuation of pump power and cell temperature, which is beneficial in enhancing the stability of laser frequency locking via polarization spectroscopy.

Acknowledgments

The authors thank Qian Jun for helpful discussion, Shen Guo-Jian for the help of manufacturing rubidium cells, and Wu Hai-Bin and Xu Da-Min for their technical support.

References

[1] Chu S 1998 *Rev. Mod. Phys.* **70** 685
[2] Phillips W D 1998 *Rev. Mod. Phys.* **70** 721
[3] Cohen-Tannoudji C N 1998 *Rev. Mod. Phys.* **70** 707
[4] Lewandowski H J, Harber D M, Whitaker D L and Cornell E A 2003 *J. Low Temp. Phys.* **132** 309
[5] Petersen M, Chicireanu R, Dawkins S T, Magalhaes D V, Mandache C, Le Coq Y, Clairon A and Bize S 2008 *Phys. Rev. Lett.* **101** 183004
[6] Poli N, Tarallo M G, Schioppo M, Oates C W and Tino G M 2009 *Appl. Phys.* B **97** 27
[7] Tiwari V B, Singh S, Mishra S R, Rawat H S and Mehendale S C 2006 *Opt. Commun.* **263** 249
[8] Millett-Sikking A, Hughes I G, Tierney P and Cornish S L 2007 *J. Phys.* B: *At. Mol. Opt. Phys.* **40** 187
[9] Reeves J M, Garcia O and Sackett C A 2006 *Appl. Opt.* **45** 372
[10] Harris M L, Cornish S L, Tripathi A and Hughes I G 2008 *J. Phys.* B: *At. Mol. Opt. Phys.* **41** 085401
[11] Wieman C and Hänsch T W 1976 *Phys. Rev. Lett.* **36** 1170
[12] Harris M L, Adams C S, Cornish S L, McLeod I C, Tarleton E and Hughes I G 2006 *Phys. Rev.* A **73** 062509
[13] Do H D, Moon G and Noh H R 2008 *Phys. Rev.* A **77** 032513
[14] Kulatunga P, Busch H C, Andrews L R and Sukenik C I 2012 *Opt. Commun.* **285** 2851
[15] Carr C, Adams C S and Weatherill K J 2012 *Opt. Lett.* **37** 118
[16] Corwin K L, Lu Z T, Hand C F, Epstein R J and Wieman C E 1998 *J. Opt. Soc. Am.* A **37** 3295
[17] Millett-Sikking A, Hughes I G, Tierney P and Cornish S L 2007 *J. Phys.* B: *At. Mol. Opt. Phys.* **40** 187
[18] Griffin P F 2005 Ph. D. Thesis "Laser Cooling and Loading of Rb into a Large Period, Quasi-Electrostatic, Optical Lattice", Durham University
[19] Kim J B, Kong H J and Lee S S 1988 *Appl. Phys. Lett.* **52** 417
[20] Javaux C, Hughes I G, Lochead G, Millen J and Jones M P A 2010 *Eur. Phys. J.* D **57** 151
[21] Yoshikawa Y, Umeki T, Mukae T, Torii Y and Kuga T 2003 *J. Opt. Soc. Am.* A **42** 6645
[22] Demtröder W 2008 *Laser Spectroscopy* (Berlin/Heidelberg: Springer-Verlag)
[23] Pearman C P, Adams C S, Cox S G, Griffin P F, Smith D A and Hughes I G 2002 *J. Phys.* B: *At. Mol. Opt. Phys.* **35** 5141